Modeling of Human Welder Response to 3D Weld Pool Surface: Part I – Principles

From the experiments, the human welder to be modeled improved the consistency of his responses to the 3D weld pool surface through the adaptation process

BY W. J. ZHANG AND Y. M. ZHANG

ABSTRACT

Understanding and modeling of human welders' response to a three-dimensional (3D) weld pool surface may help develop intelligent welding robotic systems and train welders faster. In this first effort to model human welders' behavior, a novice welder's adjustment on the welding current as a response to the 3D weld pool surface as characterized by its width, length, and convexity is studied. In this part of the paper, the human welders' behavior is analyzed from modeling's point of view. A unique, innovative machine vision system that can measure in real time the specular 3D weld pool surface under strong arc in gas tungsten arc welding (GTAW) was used to record the weld pool surface the welder observes. Experiments were conducted to train this novice welder to gain a minimal level of operation consistency such that his response to the 3D weld pool surface was not purely random. A criterion has been proposed accordingly to quantify the response consistency. Further preparation experiments were conducted to determine the time interval during which the welder responded to the weld pool surface. The resultant time interval will be used together with data from the identification experiment, specially designed to ensure modeling accuracy, to identify the welder response model in the second part of this paper.

Introduction

Skilled welders can appraise the state of weld joint penetration through their observation of the weld pool and intelligently adjust the welding parameters (e.g., current, welding speed, arc length, and torch orientation) accordingly to control the welding process for the desired state of weld joint penetration. They are sometimes preferred over mechanized welding control systems because of their sensory capabilities and ability to respond to the information they sense. However, human welders have physical limitations (inconsistent concentration, fatigue, stress, and long-term health issues), but those limitations do not exist in robotic systems or can be overcome by robotic systems. The mechanism of welders' experience-based behavior should be fully explored and utilized to develop intelligent robotic welding systems that combine intelligence and physical capabilities for next-generation manufacturing. Modeling human welders' responses, i.e., how they respond to the information they acquire through their senses, plays a fundamental role in facilitating such a development. In addition, the resultant welder response models may also be utilized to understand why less skilled welders are not performing as well as skilled welders and to help train welders faster in order to help resolve the skilled welder shortage issue the manufacturing industry is facing (Ref. 1).

Extensive studies have been done to observe the weld pool with various techniques (Refs. 2–10). Different types of information have been extracted and interpreted to describe the state of the welding process. In particular, the weld pool geometry is believed to provide valuable insights into the state of the welding process. Important information such as weld defects and penetration are contained in the surface deformation of the weld pool in the GTAW process (Refs. 11, 12). The geometry of the weld pool has been studied (Refs. 13–18) as a means of monitoring and controlling the weld joint penetration. Despite the successes in monitoring the weld pool, interpretation and modeling of the mechanism of human welders' behavior remains challenging. Up to now, there has been no literature published in this particular academic realm.

The theory of modeling for human controller dynamics has been extensively studied since the 1940s. Great progress was achieved in the 1960s and 1970s (Ref. 19), such as the linear crossover model (Ref. 20) and optimal control model (Ref. 21). The physical nature of a human operator indicates that the human controller is naturally dynamic, stochastic, nonlinear, and time varying. In this sense, the nonlinear methods were introduced to model the human action by neural networks and neuro-fuzzy or adaptive models (Refs. 22–26). Although the nonlinear methods typically improve the prediction performance to some extent, it is still very appealing to use linear models because of their convenience for analysis and design. Instead of taking the real industrial processes, most of the literature in this area took certain benchmarks as control objects, such as the pendulum and joystick. Besides, those developed models tend to be too complex to understand and difficult to be applied to practical control systems.

The goal of this first study on human welder responses is to establish and analyze dynamic models of a novice human welder's adjustment on the welding current in response to the observed 3D weld pool surface during a complete joint penetration process. Modeling welder's adjustment of other parameters such as the arc length, welding speed, and torch orientation according to the weld pool surface is the authors' future work and beyond the scope of this first study. A novice welder is studied first because the authors intend to study and follow the development of welder skills and responses.

This paper features the following sections: the principle of a human welder's behavior; a vision-based sensing system by

KEYWORDS

Human Welder's Behavior
Real-Time Measurement
3D Weld Pool Surface
Gas Tungsten Arc Welding (GTAW)

W. J. ZHANG and Y. M. ZHANG (ymzhang@engr.uky.edu) *are with the Institute for Sustainable Manufacturing and Department of Electrical and Computer Engineering, University of Kentucky, Lexington, Ky.*

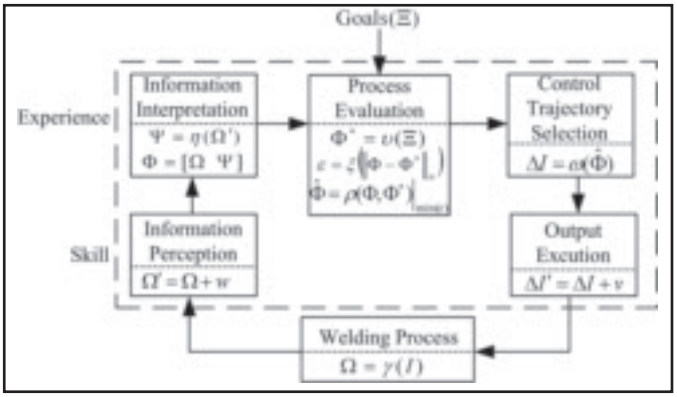

Fig. 1 — Illustration of an interpretation featuring a human welder's behavior.

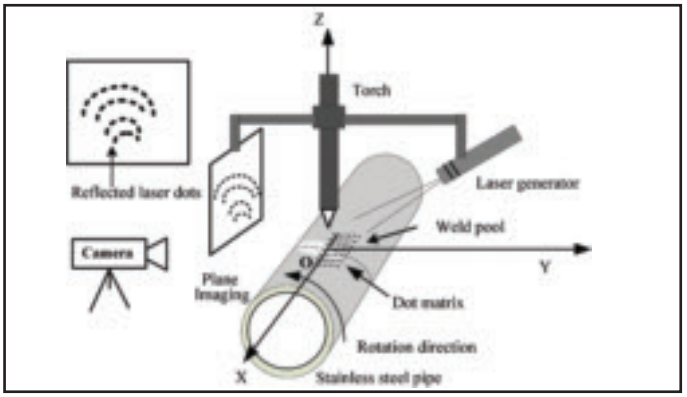

Fig. 2 — Vision-based sensing system.

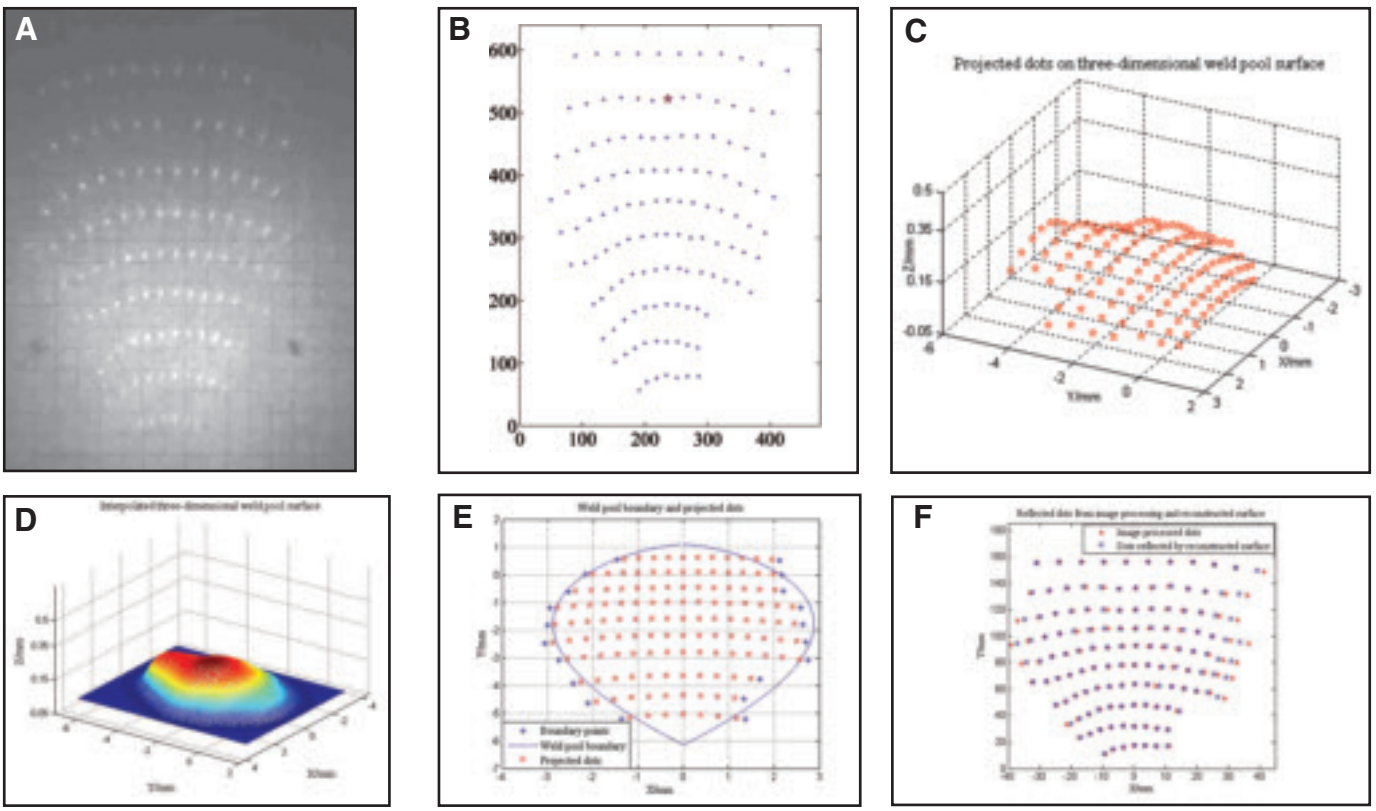

Fig. 3 — Results of image processing and 3D reconstruction. A — Captured image using the sensing system; B — resultant dots in the captured image using image processing; C — projected dots on the 3D weld pool surface; D — interpolated 3D weld pool surface; E — weld pool boundary and the projected dots; F — measured and calculated reflection pattern.

which images of the front-side weld pool are captured, processed, and reconstructed in 3D; the methods/procedures used for modeling the human welder's response in this study; the preparation experiments, including the adaptation process for the novice welder and those for step responses, are designed and conducted, and the results are presented and analyzed; the summary of this first part of this study.

Principle of Human Welder's Behavior

In this section, the principle of a human welder's behavior during welding performance is detailed. The diagram of the human welder's behavior is shown in Fig. 1. Given a certain welding task, a human welder starts with some initial estimation input I, which may include the current, arc length, and welding speed. This input is generated based on the experience of the human welder. If well trained, the human welder can generate a better guess for the target results.

After the initial input, the welder perceives necessary direct information Ω' from the weld pool. This sensing process is perturbed, in a sense of mathematical modeling, by a noise w, which might be an independent white Gaussian noise representing the randomness of the human welder. The accuracy of the sensing process or the noise level as measured by the variance of w reflects the welder's perception skill. Ω is the information that should be sensed from the welding process, which is controlled by the following welding parameters:

$$\Omega = \gamma(I) \quad (1)$$

The welder may derive indirect information ψ from the following direct information:

$$\psi = \eta(\Omega') \quad (2)$$

The process is task oriented and welder's experience based. It may involve

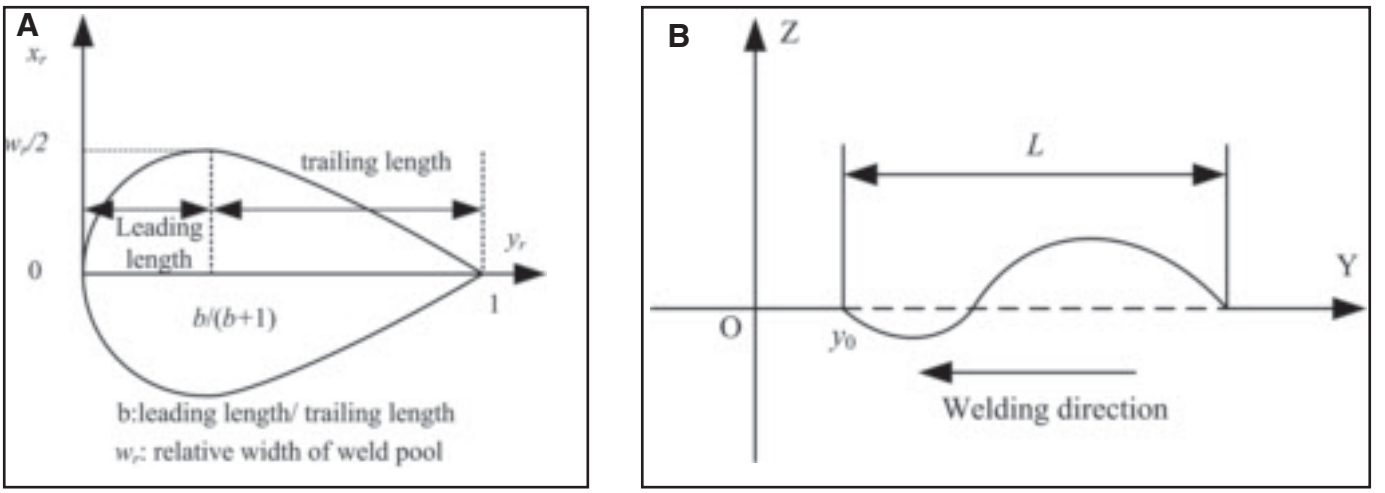

Fig. 4 — Weld pool modeling and parameters. A — 2D boundary; B — longitudinal intercepted area.

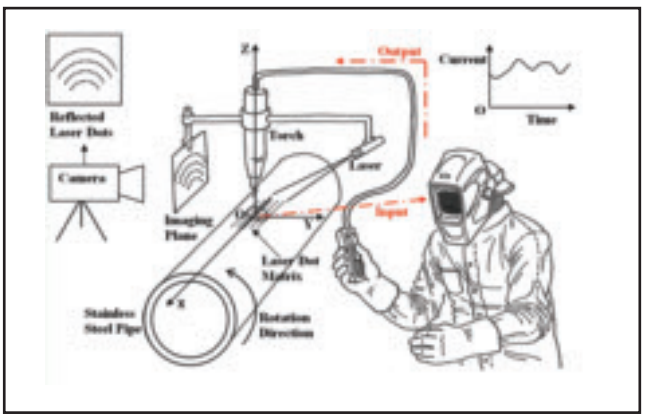

Fig. 5 — Demonstration of a manual control system featuring the GTAW process. The use of the remote control for welding current shown in the figure is for demonstration purposes only. The actual current remote control is a thumb turn knob on the torch. It adjusts the current setting for the power supply.

taking the derivative, the integral of the direct information, or the prediction of the information in the future (Ref. 26). The instant state of the welding process Φ may contain both the direct and indirect information of the welding process.

The process evaluation is the decision-making process. Given the inconsistent nature of human welder action, there may exist a certain inconsistency of welding performance even for a well-trained welder. However, skilled human welders are believed to make an optimal or nearly optimal control to minimize the error between the current and desired state of the welding process provided they are well motivated. Hence, the reactions from different skilled welders should closely match similar optimal control trajectories. In this sense, the welder first maps the goals of the welding process Ξ into the desired state of welding process Φ^* as follows:

$$\Phi^* = \upsilon(\Xi) \tag{3}$$

Then the welder evaluates the desired and instant state with some norm-based cost function, denoted in Equation 4. The optimal state for the next instant $\hat{\Phi}$ can be considered to minimize the cost function, which is shown in Equation 5.

$$\varepsilon = \xi\left(\left\|\Phi - \Phi^*\right\|_n\right) \tag{4}$$

$$\hat{\Phi} = \rho\left(\Phi, \Phi^*\right)\Big|_{\min(\varepsilon)} \tag{5}$$

Eventually, the welder maps the optimal state to the control as follows:

$$\Delta I = \omega\left(\hat{\Phi}\right) \tag{6}$$

The output execution may be considered to be perturbed by a white Gaussian noise v, which reflects the maneuvering skill of the human welder. It should be noted that the human welders' behavior depends on their skills and experiences. For the five elements of a human welder's behavior in the skill and experience levels in Fig. 1, there might be a difference in each individual element in various extents for the different welders. However, it is believed their behavior has an identical result for the combination of the five elements based on the fact that for the one welding process, different skilled welders can produce almost the same weld that meets the same requirements. Therefore, there exists a common pattern from the direct information Ω to the welder's output I, which is defined as the following equation:

$$\Delta I = F(\Omega) \tag{7}$$

The model of a human welder's behavior (Equation 7) can be considered as a combination of the five elements from "information perception" to "output execution" in Fig. 1. It is possibly nonlinear and time varying. However, it does not mean that the human welder response model cannot be identified using a linear model.

Table 1 — Experiment Parameters

	Welding Parameters	
Welding speed (mm/s)	Arc length (mm)	Argon flow rate (L/min)
1, 2	2, 5	11.8
	Monitoring Parameters	
Project angle (deg)	Laser to weld pool distance (mm)	Imaging plane to weld pool distance (mm)
35.5	24.7	101
	Camera Parameters	
Shutter speed (ms)	Frame rate (fps)	Camera to imaging plane distance (mm)
4	30	57.8

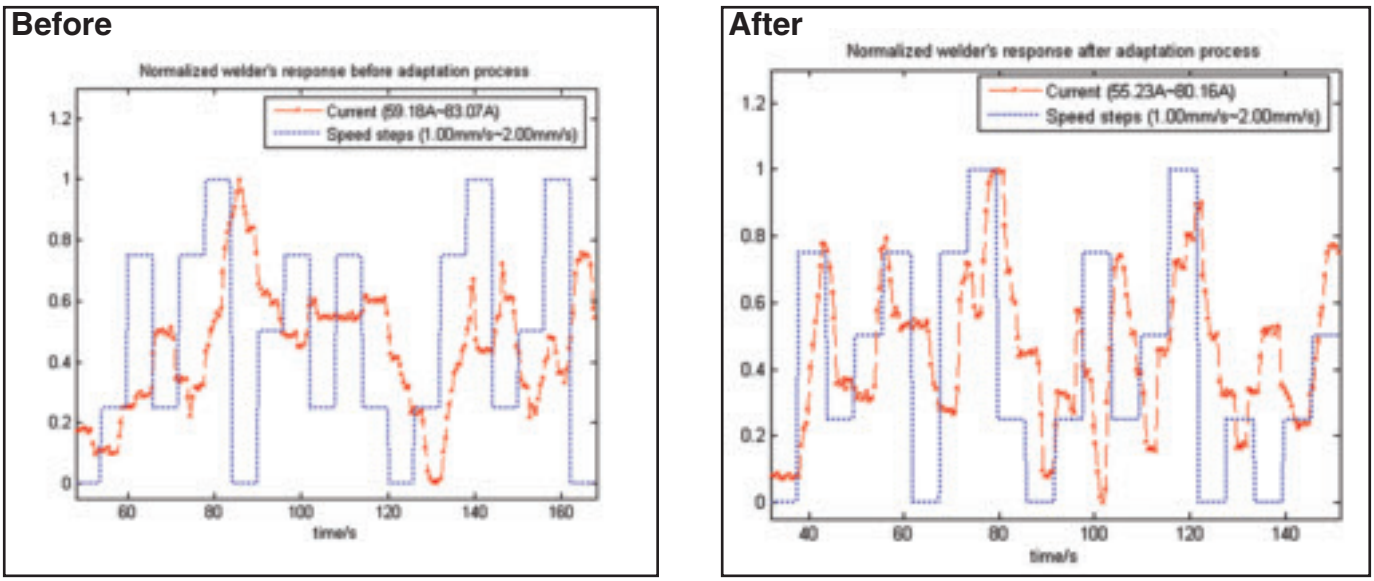

Fig. 6 — Normalized welder's responses before and after the adaptation process. Welding current and speed are plotted using the normalized scale. The range for each variable is given in each plot and corresponds to [0, 1] in the normalized scale.

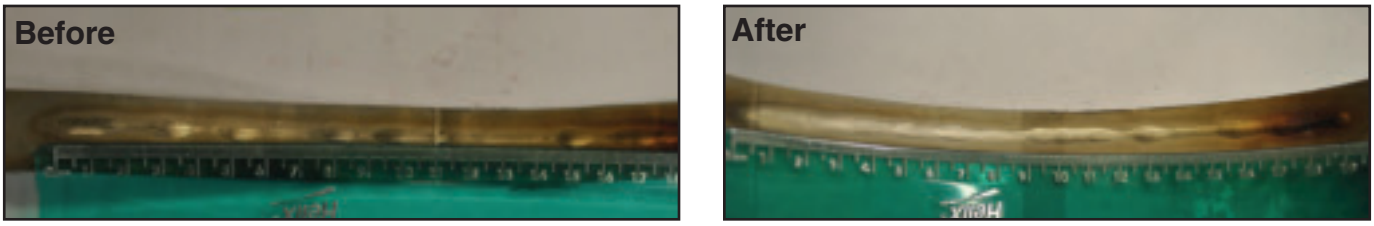

Fig. 7 — Backside weld bead appearances before and after the adaptation process. The fluctuations must exist in the weld beads because the welding speed was intentionally changed to generate fluctuating weld pools in order to examine how the welder responded to them. When making actual welds, the welding speed should not be intentionally changed and will not change in such a large range at such high speeds.

Actually, on simple manual control tasks, a linear model can well capture the human behavior (Ref. 28). This is because instead of applying a mechanistic approach to the control of the weld pool, a human welder applies a more humanistic approach that is based on partial truths (the experience) other than precise and formal truths (the physical mechanism).

This study focuses on modeling human welder's adjustments on the welding current in response to the 3D weld pool during a complete-joint-penetration welding process. The proposed model's output ΔI is the adjustment of the welding current made by the human welder. The direct information Ω, i.e., a set of characteristic parameters of the 3D weld pool geometry, is the input of the proposed model. The weld pool is thought by many as the major source to indicate the state of the welding process. It also couples with almost all the sensory signals during a welding process such as arc length (voltage), arc light intensity, and temperature. A human welder can easily acquire the geometric information of a weld pool. Therefore, it is reasonable to believe that a human welder can acquire adequate information from the weld pool surface to control the weld joint penetration.

Weld Pool Surface Characteristic Parameters

A human welder performs welding by observing the weld pool. In order to model the human welder's behavior, a vision-based sensing system is needed to emulate the vision information perception of a human welder. In this section, the setup of the sensing system is detailed. The image processing and reconstruction of the weld pool surface are briefly introduced together with the characteristic parameters of the weld pool surface used in this study. The configuration of the sensing system is shown in Fig. 2.

In order to capture the geometric information of the weld pool in 3D, a 20-mW illumination laser generator at a wavelength of 685 nm with variable focus is used to project a 19-by-19 dot-matrix-structured light pattern (Lasiris SNF-519X (0.77)-685-20) onto the weld pool region. Part of the dot matrix projected inside the weld pool is reflected by the specular weld pool surface. Because of the plasma arc impact, the surface of the weld pool is depressed and distorted in GTAW. Therefore, no matter which shape (con-

Table 2 — Experiments Conducted at One Constant Arc Length (2, 5 mm)

Step changes (mm/s)	–1.0	–0.75	–0.5	–0.25	0.25	0.5	0.75	1.0
Welding speed change (mm/s)	2.0–>1.0 2.0–>1.0 2.0–>1.0	2.0–>1.25 1.75–>1.0 2.0–>1.25 1.75–>1.0	2–>1.5 1.75–>1.25 1.5–>1.0	2–>1.75 1.75–>1.50 1.50–>1.25 1.25–>1.0	1.0–>1.25 1.25–>1.50 1.50–>1.75 1.75–>2.0	1.0–>1.50 1.25–>1.75 1.50–>2.0	1.0–>1.75 1.25–>2.0 1.0–>1.75 1.25–>2.0	1.0–>2.0 1.0–>2.0 1.0–>2.0

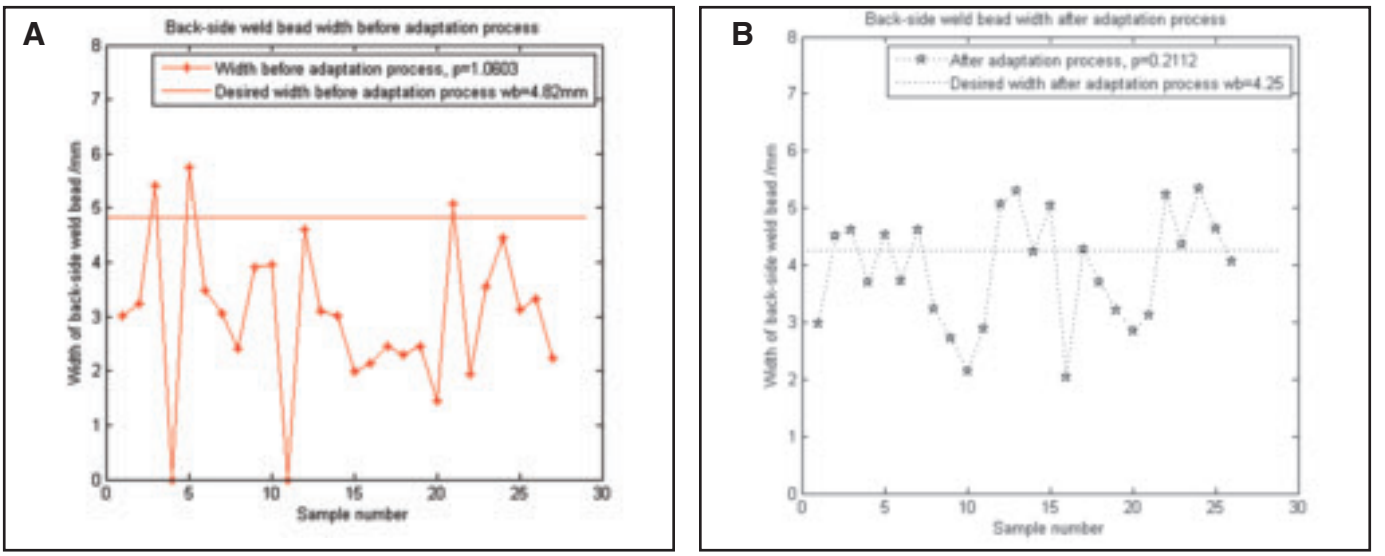

Fig. 8 — Backside weld bead widths. A — Width before adaptation process; B — width after adaptation process.

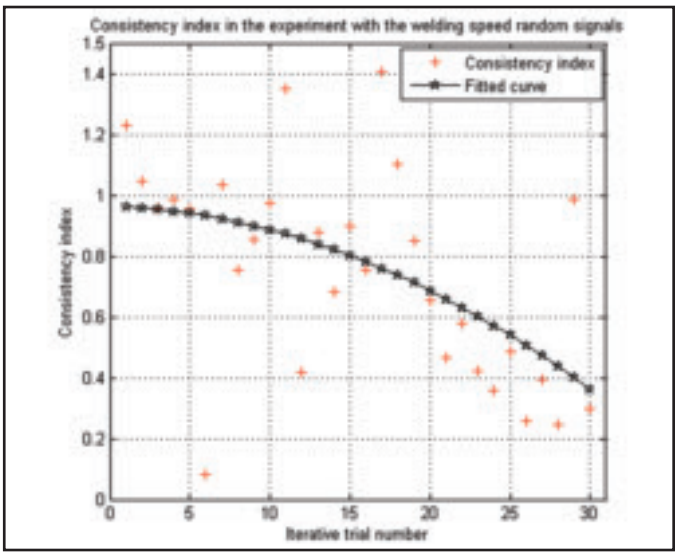

Fig. 9 — Consistency index and trajectory from 30 trials in the adaptation process.

cave or convex) the weld pool presents, the alignment of the reflected laser dot matrix is distorted by the deformed specular weld pool surface.

The distortion of the reflected dot matrix is determined by the shape of the 3D weld pool surface and contains the 3D geometry information about the weld pool surface.

In order to capture the image of the reflected dot matrix from the weld pool, an imaging plane is installed about 100 mm from the torch. A camera located behind the imaging plane is aimed directly at it. The camera captures the images of the reflected laser dot matrix from the imaging plane with a resolution 640 × 480. A bandpass filter matched to the laser wavelength is attached to the camera to block the arc radiation. A computer connects with the camera using a 9-pin 1394b interface. With a max frame rate of 200 fps at 640 × 480 resolution, the high transfer rate for camera to PC (800 M/s maximum) makes the real-time monitoring and measurement of front-side weld pool geometry in the GTAW process possible. By specific image processing and reconstruction algorithms (Ref. 7), the weld pool geometry, including the boundary and 3D surface shape, is obtained. Taking Fig. 3A, an image acquired in the imaging plane, as an example, the results of image processing and reconstruction are shown in Fig. 3B–F. The time required for image capturing, processing, and weld pool reconstruction is about 30 ms, which is fast enough for monitoring the weld pool dynamics in GTAW.

The camera behind the imaging plane shown in Fig. 2 captures the reflection image of the dot matrix from the specular weld pool surface, and an example is shown in Fig. 3A. The extracted dots in the acquired image through imaging processing are shown in Fig. 3B. The asterisk in the figure is the reference dot matching the dot at the 10th row and 10th column in the projected laser dot matrix. It facilitates matching the projected dots on the weld pool to a corresponding reflection in the acquired image. The reflection formation of dot matrix in the captured image is simply governed by the reflection law. Therefore, the 3D positions of the projected dot matrix on the weld pool surface can be determined by solving an inverse problem of the reflection law. Figure 3C shows the position of each projected laser dot on the reconstructed weld pool surface. The interpolation result of the 3D weld pool in Fig. 3D gives a more detailed view. The two-dimensional (2D) shape of the weld pool in a oxy plane is shown in Fig. 3E. The pentagrams are the reflected laser dots, and the stars are the boundary dots of the weld pool. The boundary of the weld pool is then fitted using the algorithm from literature (Ref. 29).

The accuracy of the measurement of the 3D weld pool surface can be verified by the match between the calculated reflection image from the reconstructed weld pool surface and extracted reflection image from imaging processing. The comparison of the two reflection images is shown in Fig. 3F. The stars are the reflected dots obtained from the captured image in the experiment, and the pentagrams are the dots reflected by the reconstructed weld pool from the simulation. The match of the two reflected patterns verifies the accuracy of the reconstruction scheme.

As the skilled welder performs welding by assessing the weld pool surface, the welder would take certain characteristic parameters of the surface as the indication of complete joint penetration. In this sense, the parameters selected in this study to characterize the weld pool front-side geometry are the length, width, and convexity of the weld pool. According to the description of the weld pool boundary in literature (Ref. 29), the 2D weld pool is shown Fig. 4A. The 2D parametric model of the weld pool is presented in Equation 8. The length is the distance from the head

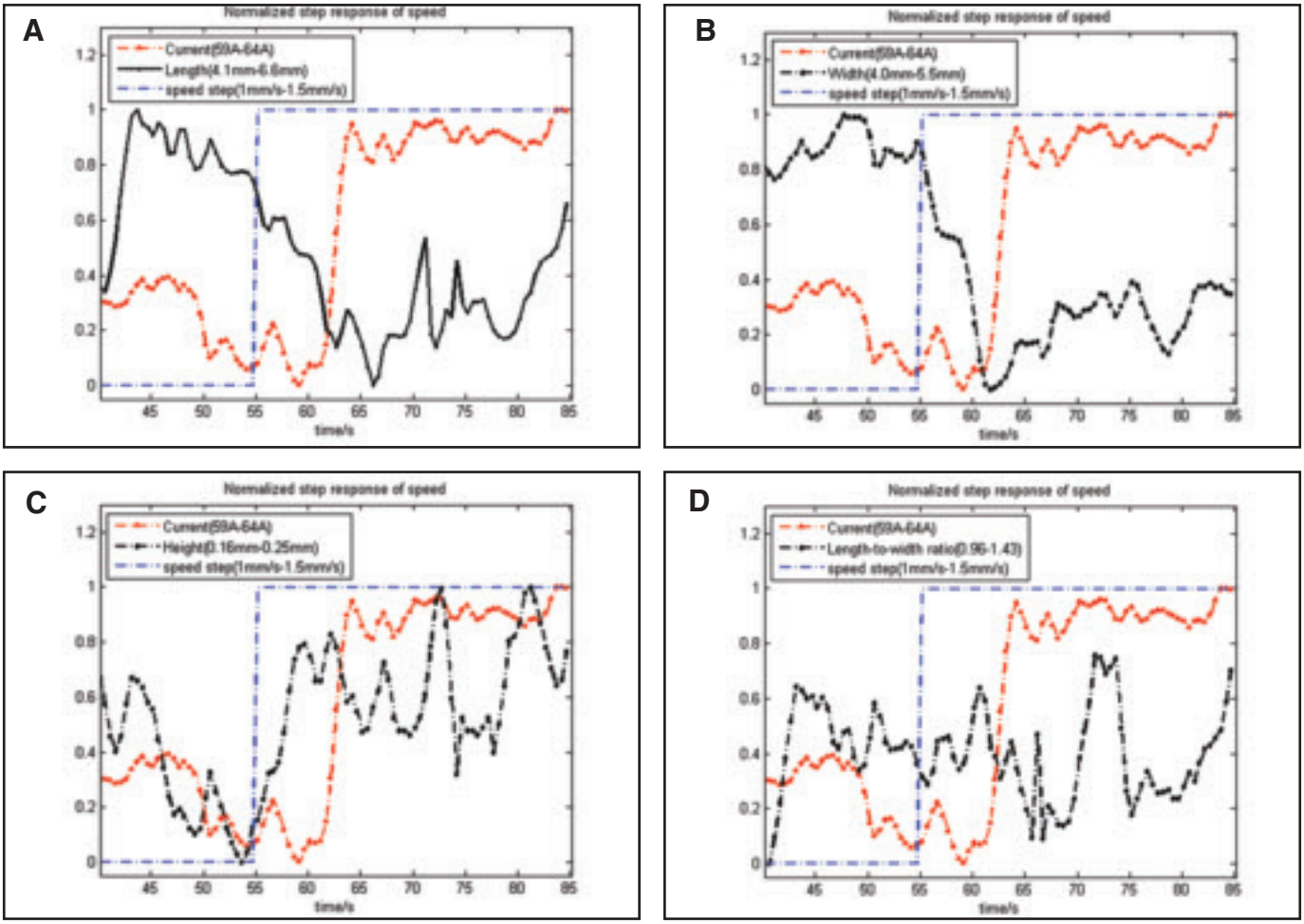

Fig. 10 — Normalized step response to welding speed. All variables are plotted using the normalized scale. The range for each variable is given in each plot and corresponds to [0, 1] in the normalized scale. A — Weld pool length; B — weld pool width; C — weld pool convexity; and D — length-to-width ratio.

to the tail of the weld pool. The width of the weld pool is calculated based on the parametric model and length, as shown in Equation 9. Figure 4B shows the longitudinal intercepted area of the weld pool in oxy plane. The convexity is defined as the intercepted area divided by the length of the weld pool.

$$x_r = \pm a y_r^b (1 - y_r), (a > 0, 1 \geq b > 0) \quad (8)$$

where $x_r = x/L$, $y_r = y/L$, and L is the length of the weld pool.

$$w = w_r \times L = 2aL\left[\frac{b}{1+b}\right]^b \left(\frac{b}{1+b}\right) \quad (9)$$

Methods of Studies

The ability to measure the weld pool surface in real time provides a capability to record the 3D weld pool surface. Further, the responses the human welder made to the 3D weld pool surface can be recorded. Using the 3D weld pool surface as the inputs and responses as the outputs, a model can be established to correlate the outputs to the inputs and to model how the human welder responds to the 3D weld pool surface. However, a successful identification of a meaningful model requires appropriate preparations.

First, the 3D weld pool surface as measured is represented by a large set of 3D coordinates. This form of representation is not a form a human welder processes. Hence, we have proposed the three characteristic parameters to represent the 3D weld pool surface above.

Second, the response of a welder to the 3D weld pool surface could vary during the operation. A skilled welder is expected to respond to the 3D weld pool surface relatively consistently. If the response of a welder to the 3D weld pool surface is purely random, modeling his responses would not lead to meaningful results, and the modeling accuracy would be extremely poor. Hence, the welder to be modeled needs to possess minimal skills

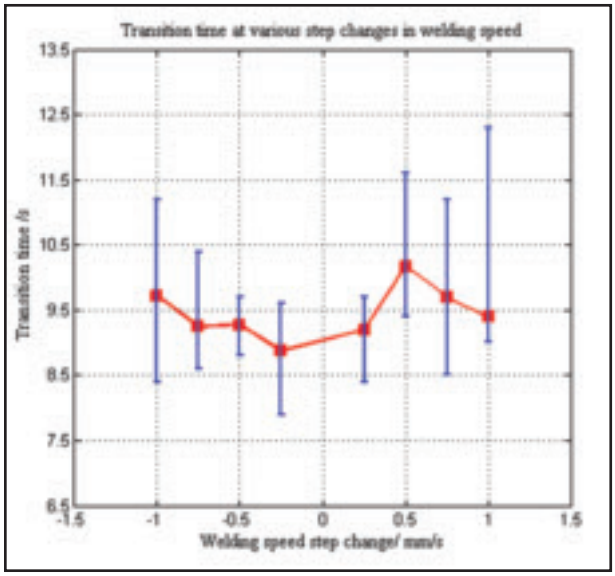

Fig. 11 — Transition times in different experiments.

such that he can respond to the 3D weld pool surface consistently. To this end, the welder is required to practice for improving his consistent welding performance to a minimally acceptable level.

Third, modeling the responses of the welder to the 3D weld pool surface is to establish a model that correlates the welder responses (model output) to the characteristic parameters (inputs) of the 3D weld pool surface. It is true that we already have the measurements for the outputs and inputs, and can use a parameter estimation method such as the least squares method to estimate the model coefficients. However, we expect that the response of the human welder to the weld pool surface is a dynamic process. That is, the welder may make the adjustments on the welding parameters not only based on the weld pool surface he just observed but also those observed earlier. Further, it is unlikely that the welder may respond to the change in the weld pool surface immediately. There must be a time delay in his response. As a result, we should be at the position to determine the time intervals within which the characteristic parameters should be included in the model to test their significance for their effect on the response. To this end, we propose to conduct step response experiments that can allow us to easily see the delay in welder response and time ranges the welder may remember, and use corresponding weld pool surfaces to make the adjustments.

The data from the step response experiment are suitable to help easily identify the time delay and welder response time intervals. However, such experiments are not most suitable to produce data that can be used to fit the model accurately. Hence, further experiments will be designed and conducted to obtain data for the estimation of the model coefficients to accurately model the welder's response.

The preparation experiments and analysis will be performed in the next section to improve the consistency of the response of the human welder being modeled and determine the time intervals of weld pool surface to which he may respond. Accurately modeling the welder's response, including design of further experiments and data analysis, will be done in the second part of the paper.

Preparation Experiments and Results

Experimental Method

In this subsection, the method for the manual GTAW experiments is introduced, and experimental parameters used are specified. In this first study on human welder response, the human welder only adjusts the welding current based on his observation of the 3D weld pool surface. Other parameters, including the welding speed, arc length, and torch orientation that may be adjusted by a human welder in a typical manual welding process are not adjusted. To this end, an experimental method illustrated in Fig. 5 is proposed.

In this experimental method, pipes are rotated and butt joint welded using direct current electrode negative (DCEN) GTAW at 12 o'clock without filler metal. The human welder observes the weld pool and adjusts the welding current using an amperage remote control installed on the torch. The 3D weld pool surface being observed by the human welder is also simultaneously measured by the vision system, and its characteristic parameters are recorded together with the adjustment made by the human welder on the welding current. Modeling of the human welder's response to the 3D weld pool surface is to correlate the recorded adjustment on the current to the recorded characteristic parameters.

The pipe used in this study is 4-in. nom. stainless T-304/304L Schedule 5. The pipe rotates during the experiment while the torch, imaging plane, laser structured light generator, and camera are fixed in the space. The rotation speed and up-down motion of the torch are controlled by a computer to achieve required welding speed and arc length. In all the experiments conducted in this study, the welding speed varied within the range (1, 2 mm/s), and the arc length was set constant for each experiment in (2, 5 mm). The current was controlled by the human welder. Other experimental settings are shown in Table 1.

Improvement on Response Consistency

The randomness/inconsistency of the human welder's performance may make this response model vary in both the structure and parameters. In order to minimize the inconsistency, an adaptation process is necessary for the human welder to go through a series of iterative trials to adapt to the particular welding process in this study. A criterion is then required to evaluate the consistency of performance for the human welder in the adaptation process. It is known the human welder can estimate the performance based on the appearance of the backside weld bead. In this sense, a simple consistency index is defined in this study to evaluate the following performance of the human welder:

$$p_i = \frac{1}{N}\sum_{k=1}^{N}\left(w_b^k - w_b^*\right)^2 \Big/ w_b^* \qquad (10)$$

where p_i is the consistency index for the human welder in the i^{th} trial, and N is the number of the sampled data of the backside weld bead width in the trial. $w^k{}_b$ is the k^{th} sample of the backside weld bead width in this i^{th} trial. $w^*{}_b$ is the desired width of the backside weld bead the human welder is supposed to produce. Compared with the convexity of the backside weld bead, the backside width is more direct to indicate the consistency of the welder's performance. A reduced index value implies improved consistency.

The adaption process is a preparation for the human welder to improve the consistency of the welding so that the welder will perform well in the experiments designed for the modeling of his dynamic response. In this sense, the experiments in the adaptation process need to be designed similar to those for the dynamic responses of the human welder. In order to successfully model the dynamic responses, the frequency span of the designed input (the characteristic parameters of weld pool geometry) is required to be wide enough. Ideally, the input should be random signals with sufficient high orders. However, the variation of a weld pool cannot be generated in a designed random form. Instead, the random signals of the welding speed are applied to the process in this study, and the weld pool geometry is expected to vary in a random manner.

In the adaptation process, five welding speeds are used: 1, 1.25, 1.5, 1.75, and 2.0 mm/s. For each practice in the process, the welding speed was randomly varied among the five values with a 6-s time interval for each change. Before the random welding speed signals were excited, there was an 18-s period at the beginning of each practice such that the human welder controlled the welding process to the complete-joint-penetration state as the weld pool approached a desired dimension. The duration for the random welding speed signals is 120 s. The arc length was set constant for each practice in (2, 5 mm), i.e., 2, 3, 4, and 5 mm. There were 30 practices in the adaptation process, approximately evenly distributed at different arc lengths (7 trials at both 2 and 5 mm arc length, and 8 trials at 3 and 4 mm arc length).

Since there was an 18-s period at the beginning of each experiment, the width of the backside weld bead at the steady state of this period can be considered as the desired width $w^*{}_b$ in Equation 10. The consistency index is expected to be reduced after iterative practices in the adaptation process such that the randomness of the human welder can be minimized in the proposed model of a human welder's behavior.

Figure 6 shows the two normalized welder's responses before and after the adaptation process, respectively. The range of each variable, i.e., from the min-

imal to the maximal value, is linearly mapped to the range [0 1] that follows:

$$x_N = \frac{x - x_{\min}}{x_{\max} - x_{\min}} \quad (11)$$

where x_N is the normalized value of x, $x_{\min}$ and $x_{\max}$ are the minimal and maximal value of x. The current controlled by the welder is adjusted according to the geometry of the weld pool surface, which is varied by the random welding speed. Figure 7 shows the difference of the two backside weld bead appearances from the two corresponding experiments before and after the adaptation process. Without any practice, it is hard for the human welder to maintain the weld pool geometry constant in the experiment in which the geometry varies greatly along with welding speed random signals. After the adaptation process, the human welder can better maintain the weld pool geometry, and the width of the backside weld bead is more consistent than the one before the adaptation process. The improvement in the consistency in the backside bead width is significant.

It should be noted that the time stamps do not start from zero in Fig. 6 and other figures about the welder's response in the following sections. First, this is because there was a fixed time interval at the beginning of each experiment for the welding process to approach the desired complete-joint-penetration state controlled by the welder. The variation of the weld pool geometry in that period is not the interest in this study and not shown in the figures. Second, the timer used to record data started before the human welder's operation in the experiments. In this way, the time duration, from when the timer started to when the welder began to weld, varied with each experiment. Therefore, the time stamp varies case by case. Nevertheless, it does not in any way affect the records of the weld pool geometry, human welder's behavior, or any other results presented in this study.

For each trial in the adaptation process, the backside weld bead width was measured. To balance between the simplicity and accuracy of the measurement, the width was sampled every 5 mm along the weld bead. In this way, the measurements for the width of the backside weld bead from the two experiments shown in Fig. 7 are obtained in Fig. 8 with A and B for before and after the adaption, respectively. While the consistency index in Fig. 8A is 1.0603, it reduces to 0.2112 after practices as shown in Fig. 8B. The improvement of the welder's consistency is significant.

Figure 8 shows the improvement achieved by the adaptation. The entire adaptation process consists of 30 trials with random welding speed at different arc lengths. The consistency indexes for all the trials in the adaptation process are shown in Fig. 9. The crosses are the calculated indexes; the curve is the fitted index. The fitted index demonstrates that the index reduces from around 0.98 to about 0.35 gradually. The progress of the welder's gradual improvement during the adaptation is clearly shown.

Response Intervals

After iterative practices in the adaptation process, experiments with the step signals of the welding speed were conducted to study the step responses of the human welder. In those experiments, the welding speed varied in the range from 1 to 2 mm/s with various possible change steps as follows: ±0.25, ±0.5, ±0.75, and ±1 mm/s. Each step signal lasted 30 s, which was long enough for the human welder to perceive the variation of the weld pool, and then adjust the current until the weld pool turns back to the desired steady state again. Before the step input was excited, there was a 15-s period at the beginning of each experiment for the human welder to control the weld pool to grow to the desired dimension.

Table 2 shows the set of experiments for step responses that were conducted repeatedly at each arc length in (2, 5 mm), i.e., 2, 3, 4, and 5 mm. In order to evenly distribute the experiment along the step changes, some identical experiments were conducted repeatedly, such as the one with welding speed changing from 2.0 to 1.0 mm/s, which were conducted three times at each arc length.

Figure 10 shows variations of weld pool geometry and the step responses of the welder in one of the experiments in which the welding speed changed from 1 to 1.5 mm/s. The arc length is 3 mm. It is found that the weld pool geometry starts to change immediately after the step input. Its size reduces distinctively as the length decreases from 5.85 to 4.85 mm and the width drops from 5.35 to 4.3 mm. The welder underestimated the effect of the welding speed on the size of the weld pool. Therefore, the current was not increased enough by the welder to maintain the same dimension of the weld pool as it was before the step change was made.

It has been found that the welding speed has significant influence on the size of the weld pool, while its effect on the weld pool appearance (length-to-width ratio) is slight (Ref. 30). In this experiment, it is the welding speed other than the current controlled by the human welder that has a leading influence in determining the weld pool geometry. The length and width are changed approximately proportionally. Therefore, the length-to-width ratio shown in Fig. 10D does not change significantly after the step change in the welding speed in this experiment. As the welding speed increases, the heat input of the weld pool is significantly reduced, and the current increased by the human welder does not fully compensate for the loss of the heat input into the weld pool. The decrease of the heat input caused the convexity of the weld pool to increase as can be seen in Fig. 10C.

In this experiment, the step change in the welding speed was generated at 54.7 s, and the weld pool turned to steady again at 63.7 s, the transition time for the convexity and the width is 7.5 s, while it is around 8.5 s for the length to turn back to steady state. This is because the reduced trailing angle caused by the welding speed step change slows down the decreasing rate of weld pool length. There is about a 3-s delay before the welder starts to increase the current. Within this period, the length of the weld pool reduces about 1.00 mm, the width drops about 1.05 mm, and the convexity increases about 0.1 mm. Based on the perceivable variation of weld pool geometry, the welder is believed to adjust the current based on the observation on the changes of the weld pool.

The welder's response to the change in the weld pool geometry may differ. The experimental parameters shown in Table 2 are used to conduct experiments at different arc lengths in (2, 5 mm). The resultant transition times are shown in Fig. 11. (The longest time is taken as the process's transition time if the three characteristic parameters have different transition times.) The square and error bar for each step change in the figure is the mean value, and the range of the transition times from the experiments conducted with this particular welding speed step change under various arc lengths.

As can be seen in Fig. 11, the transition time range is different at different step changes. There are some abnormally long transition times at some step changes. It was observed in some experiments after the step change was applied, the welder adjusted the current several times until the weld pool returned back to the steady state. However, the average of all the resultant transition times is about 8.7 s. The maximal variation is about 3 s shown at speed step change 1 mm/s. The transition times are approximately independent of the welding speed changes. At the meantime, the time delay of the welder, i.e., the period from the step change application time to the time the welder begins to react is about 1 to 3 s. No significant difference in the time delay is found among the different arc lengths or step changes. The human welder only starts to adjust the current when perceivable changes in the weld pool geometry are observed.

Summary

In the first part of the study for model-

ing human welder's behavior, the principle of a human welder's behavior is detailed. A vision-based sensing system is used to real-time record the human welder's behavior and the 3D weld pool geometry that is characterized by three parameters — the length, width, and surface convexity of the weld pool. The material used in the experiments was stainless steel pipe (4-in. nom. stainless T-304/304L Schedule 5). The arc length and welding speed were within (2, 5 mm) and (1, 2 mm/s), respectively. Under those conditions, the preparation experiments including those for the welder to improve the response consistency and those for the welder's step responses were designed and conducted. As can be seen from the experiments, the human welder to be modeled improved the consistency of his response to the 3D weld pool surface through the adaptation process. Further, the average transition time was 8.7 s, and the welder response delay was from 1 to 3 s.

The improved consistency is needed in order to model and analyze the response of a human welder. The knowledge of the transition time and response delay is needed to determine the time period within which the 3D weld pool surfaces need to be included in a model to predict the welder's adjustment on the welding current. With the improved consistency and knowledge about the transition time and response delay, the next part of the paper will have the foundation to model the welder's response. However, while the step welding speed change experiments in this part of the paper can be easily used to determine the transition time and response delay, dynamic variations in the welding speed need to be applied to generate more dynamic weld pools in order to identify the welder's response accurately. The next part of the paper is devoted to design dynamic experiments and use/analyze the data from dynamic experiments to model and understand the welder's response.

Acknowledgments

This work is funded by the National Science Foundation under grant CMMI-0927707. We wish to thank Yi Lu and YuKang Liu for their assistance on experiments and graphics as well as Lee Kvidahl for his technical guidance on manual pipe welding.

References

1. Uttrachi, G. D. 2007.Welder shortage requires new thinking. *Welding Journal* 86(1): 6.

2. Richardson, R. W., and Edwards, F. S. 1995. Controlling GT arc length from arc light emissions. *Trends in Welding, Proceedings of the 4th International Conference*, pp. 715–720.

3. Li, P. J., and Zhang, Y. M. 2011. Precision sensing of arc length in GTAW based on arc light spectrum. *Journal of Manufacturing and Science Engineering* 123: 62–65.

4. Stecker, S. D. 1996. Characterization and application of weld pool oscillation phenomenon for penetration control of gas tungsten arc welding. MS thesis, The Ohio State University, Department of Welding Engineering.

5. Hartman, D. A., DeLapp, D. R., Barnett, R. J., and Cook, G. E. 1998. A neural network/fuzzy logic system for weld penetration control. *Trends in Welding Research, Proceedings of the 5th International Conference*, pp. 1096–1101.

6. Balfour, C., Smith, J. S., and Al-Shamma'a, A. I. 2006. A novel edge feature correlation algorithm for real-time computer vision-based molten weld pool measurements. *Welding Journal* 85(1): 1-s to 8-s.

7. Song, H. S., and Zhang, Y. M. 2009. Error analysis of a three-dimensional GTA weld pool surface measurement system. *Welding Journal* 88(7): 141-s to 148-s.

8. DeLapp, D. R. 2005. Observations of solidification and surface flow on autogenous gas tungsten arc weld pools. PhD dissertation, Vanderbilt University.

9. Zhang, S. B., Sun, D., and Xu, P. 2003. Trackless welding of large steel structures. *Welding Journal* 82(7): 32–36.

10. Zhang, W. J., Liu, Y., Wang, X., and Zhang, Y. M. 2012. Characterization of three-dimensional weld pool surface in GTAW. *Welding Journal* 91(7): 195-s to 203-s.

11. Lin, M. L., and Eagar, T. W. 1985. Influence of arc pressure on weld pool geometry. *Welding Journal* 64(6): 163–169.

12. Rokhlin, S. I., and Guu, A. C. 1993. A study of arc force, pool depression, and weld penetration during gas tungsten arc welding. *Welding Journal* 72(8): 381–390.

13. Zhang, Y. M., Li, L., and Kovacevic, R. 1995. Monitoring of weld pool appearance for penetration control. *Proceedings of the 4th International Conference*, pp. 683–688.

14. Kovacevic, R., and Zhang, Y. M. 1996. Sensing free surface of arc weld pool using specular reflection: Principle and analysis. *Journal of Engineering Manufacture, Proceedings Part B*.210(B6): 553–564.

15. Kovacevic, R., and Zhang, Y. M. 1996. Monitoring of weld joint penetration based on weld pool geometrical appearance. *Welding Journal* 75(10): 317–329.

16. Zheng, B., Wang, H. J., Wang, Q. I., and Kovacevic, R. 2000. Control for weld penetration in VPPAW of aluminum alloys using the front weld pool image signal. *Welding Journal* 79(12): 363-s to 370-s.

17. Chen, W. H., and Chin, B. A. 1990. Monitoring weld penetration using infrared sensing techniques. *Welding Journal* 69(5): 181-s to 185-s.

18. Bentley, A. E., and Marburger, S. J. 1992. Arc welding penetration control using quantitative feedback theory. *Welding Journal* 71(11): 397-s to 405-s.

19. Gaines, B. 1969. Linear and nonlinear models of the human controller. *International Journal of Man-Machine Studies*. pp. 1333–360.

20. McRuer, D., Graham, D., Krendel, E., and Reisener, W. 1965. Human pilot dynamics in compensatory systems. Technical report. AFFDL-TR-65-15, Air Force Flight Dynamics Laboratory, Wright-Patterson AFB, Ohio.

21. Kleiman, D. L., Baron, S., and Levison, W. H. 1970. An optimal model of human response, Part 1. Theory and validation. *Automatica* 6: 357–369.

22. Chen, L. K., and Ulsoy, A. G. 2000. Identification of a nonlinear driver model via narmax modeling. *Proceedings of American Control Conference*, pp. 2533–2537.

23. Tsuji, T., and Tanaka, Y. 2005. Tracking control properties of human-robotic systems based on impedance control. *IEEE Transactions on Systems, Man, and Cybernetics — Part A: Systems and Humans* 35(4): 523–535.

24. Itoh, E., and Suzuki, S. 2005. Nonlinear approach for human internal models: Feed forward and feedback roles in pilot maneuver. *Systems, Man, and Cybernetics. 2005 IEEE International Conference* 3: 2455–2462.

25. Delice, I. I., and Ertugrul, S. 2007. Intelligent modeling of human driver: A survey. *2007 IEEE Intelligent Vehicles Symposium*. pp. 648–651.

26. Ertugrul, S. 2008. Predictive modeling of human operators using parametric and neuro-fuzzy models by means of computer-based identification experiment. *Engineering Applications of Artificial Intelligence* 21: 259–268.

27. Wickens, C. D., and Carswell, C. M. 1997. Information processing. Salvendy, G. (ed.) *Handbook of Human Factors and Ergonomics*, Wiley, New York, pp. 89–129.

28. Antunes, R., Fernando V. C., and Hermínio, D. R. 2011. A linear approach towards modeling human behavior. *IFIP Advances in Information and Communication Technology* 349: 305–314.

29. Zhang, Y. M., and Li, L. 1997. Dynamic estimation of full penetration using geometry of adjacent weld pools. *Journal of Manufacturing Science and Engineering* 19: 631–644.

30. Kovacevic, R., Cao, Z. N., and Zhang, Y. M. 1996. Role of welding parameters in determining the geometrical appearance of the weld pool. *Journal of Manufacturing Science and Engineering* 118: 589–595.